A Mathematical Model of the First Steps of Tumour-Related Angiogenesis: Capillary Sprout Formation and Secondary Branching

M.E. Humphreys and M.A.J. Chaplain

School of Mathematical Sciences,

University of Bath,

Bath BA2 7AY.

Tel: (+44) 0225 826242

FAX: (+44) 0225 826492

e-mail: meh, majc@maths.bath.ac.uk

Abstract

The growth of a solid tumour is dependent on an adequate supply of nutrients. A tumour can establish a blood supply by inducing neighbouring blood vessels to sprout and grow towards it, a process known as angiogenesis. The tumour cells may secrete a number of diffusible chemicals which stimulate endothelial cells (EC) to proliferate and to rearrange themselves into capillary tubes or sprouts. In this paper we focus firstly upon the early stage of angiogenesis wherein the EC group together in the parent vessel to form the initial capillary sprout buds. A mathematical model for the formation of the capillary buds is presented which focuses on the potential role

that haptotaxis may play. In the second part of the paper we turn attention to the EC within the growing and developing capillary sprouts as they migrate towards the tumour cells. Once again the potential role of haptotaxis is focussed upon.

1 Introduction

The growth of most solid tumours takes place in two stages [19]. In the first stage, the tumour is avascular, that is it does not have a network of capillary vessels supplying it with nutrients. During this avascular stage, the tumour may be considered as being roughly spherical and consists of a central necrotic core surrounded by a layer of proliferating cells. At this stage the tumour is small enough (1-3mm in diameter) to take in nutrients and expel waste products by diffusion alone. However diffusion is not sufficient to support any continued growth of the tumour. This is because the tumour consumes nutrients at a rate proportional to its volume whereas the supply of nutrients is proportional to its surface area. The avascular tumour can become dormant and there is an indefinite period for which growth stops.

The inadequacy of diffusion as a means of transportation of vital nutrients to a cell has been demonstrated, for example, by LaBarbera and Vogel (1982) [18]. Suppose we have a spherical cell of radius r with volume $V = 4\pi r^3/3$ and surface area $S = 4\pi r^2$. Suppose the concentration of a given substance at the cell surface is c_0 and that the cell uses up the substance completely so that at $r = 0$, $c(r,t) = 0$ where c is the concentration of the substance. The gradient of substance will then be c_0/r. Hence the total diffusive flux through the cell surface will be

$$J = D\frac{c_0}{r}S = 4\pi D c_0 r,$$

where D is the diffusion coefficient. The rate at which the substance is depleted up will be proportional to the cell's volume. If τ is a constant representing the time it takes for the substance to be used up completely then

$$\text{rate at which substance used} = \frac{4\pi r^3}{3\tau}.$$

Hence,

$$\frac{\text{rate of supply}}{\text{rate used}} \simeq \frac{3Dc_0\tau}{r^2}.$$

In order to meet the demands of the cell the rate of supply of the substance must be greater or equal to the rate at which the substance is used, i.e. the ratio must be greater than 1. Thus

$$c_0 > \frac{r^2}{3D\tau}.$$

So the external substance concentration must be at the very least proportional to the radius of the cell squared. This is unrealistic if the radius is large and hence the structure of avascular tumours with the necrotic core.

During the second stage of growth, the tumour becomes vascular, that is, it is penetrated by capillary vessels. A vascularized tumour can grow exponentially and there is the possibility of both invasion and metastasis [9] . Vascularization is realized by a process known as angiogenesis which is the formation of blood vessels. Angiogenesis also occurs during physiological processes such as embryonic development, or pathological processes such as wound healing, rheumatoid disease and tumour growth (see references in [25]).

Various techniques have been developed in order to examine the cascade of events that lead to neovascularization. For example, the cloning of capillary endothelial cells in culture is a method used for studying angiogenesis *in vitro* [10], [15] . As *in vitro* studies can only generalize about angiogenesis, *in vivo* studies are also employed in order to explore the specifics of tumour-induced angiogenesis. The corneal micropocket [22] and the hamster cheek pouch chamber [14] are just two of the methods used to study angiogenesis *in vivo.*

The lining of many vessels such as veins and small lymphatic vessels are formed from a monolayer of endothelial cells (EC). The EC lie upon a continuous basement membrane (or basal lamina) and are in close contact with their neighbours. EC play an important role in angiogenesis. In fact it has been shown *in vitro* that EC can construct capillary networks unaided by other cell types [10].

Angiogenesis is initiated by the release of angiogenic factors from the tumour, though it is not known what triggers this activity. There are two types of angiogenic factors, those that act directly on the EC and those that induce other cells into producing factors which act on the EC [10] , [11]. Angiogenic factors induce one or more of the following activities in the EC:

1. the secretion of proteases and collagenases by the EC which degrade the basal lamina and the extracellular matrix.

2. the migration of EC towards a chemotactic stimulus.

3. proliferation of EC.

For successful tumour vascularization, all three events must be carefully orchestrated. In recent years several angiogenic factors have been identified. A summary of these factors can be found in Folkman and Klagsbrun (1987) [11]. The suggestion is that several angiogenic factors act together, either directly or indirectly, to promote angiogenesis. We will now describe the above activities in more detail.

The tumour releases angiogenic factors (or TAF) which diffuse into the surrounding tissue. The first reaction to this stimulus is that the EC in the neighbouring vessels and nearest to the chemical source start to alter their structure. The cells thicken and finger-like protrusions can be observed on the abluminal surface [1] , [25]. Cell associated proteases degrade the basement membrane so that the EC loosen their contacts with their neighbours. Stimulated by the TAF the EC begin to migrate [35]. The EC accumulate in the region where the concentration of angiogenic factors has first reached a threshold level [25]. The vessel wall begins to bulge as EC pile up to form sprouts. The basement membrane does not contain gaps large enough to allow EC passage into the extracellular matrix beyond the vessel wall. Therefore the EC secrete proteases and collagenases which dissolve the basal lamina and the surrounding extracellular matrix enabling the capillary sprout to grow towards the tumour [16].

The capillary sprouts begin to grow in length by recruiting EC from the parent vessel. At some distance from the tip of the sprout EC begin to proliferate. There is evidence that migration and mitosis are independent events and that separate angiogenic factors are required to stimulate these activities of EC [8], [25] ,[35] . The first stages of angiogenesis can be performed without cell proliferation [29], mitosis occurring after the capillary sprouts have started to grow. However, proliferation is essential for the completion of angiogenesis as gaps will develop in the parent vessel resulting in abnormal permeability [1].

The EC in the outgrowing sprouts start to reassociate with each other. The development of intracellular lumen, where vacuoles appear within the EC, and intercellular lumen, where vacuoles appear between the outgrowing sprouts, leads to the formation of tube-like structures [17]. Branches form in a similar way whereby an intracellular vacuole becomes Y or T shaped before fusing with the primary lumen [10]. Initially the sprouts are parallel with each other vessel but tend towards each other as they elongate. Neighbouring sprouts will eventually fuse together at their tips to form loops (anastomoses). This signals the beginning of circulation of blood. It is essential that there is a flow of blood through the tumour since an effective system for transporting waste products away from the tumour is vital. As the vessels mature, the EC resynthesize a basal lamina in order to restore continuity. The looped vessels may bud or loops may fuse with other loops until a complex network of vessels develop. Finally this network penetrates the tumour, providing it with the circulatory system and the supply of nutrients that it requires for growth. In order to support continued growth the tumour's vascular system persistently remodels itself. Hence angiogenesis is an on-going process, continuing indefinitely until the tumour is removed or killed, or until the host dies.

Initially the EC are uniformly distributed along the walls of the parent vessel. The release of diffusible substances from the tumour triggers an angiogenic response in the EC. The EC become mobile and form clusters of cells which are the beginning of the buds. These buds will eventually sprout and will form the primary capillary vessels in the tumour's vascular system. There is clear experimental evidence that the mechanism by which the cells move involves haptotaxis, i.e. the cells move up an adhesive gradient, especially in the early stages. Studies have shown that compounds such as fibronectin are secreted by the EC during the angiogenic process [5], [25] and that fibronectin increases cell to cell and cell to matrix adhesiveness [6] , [34] . It can be supposed that fibronectin aids angiogenesis by directing migration [6] , [5] ,[25] , [33] . Chemotaxis is also involved in angiogenesis, but we will focus our attention on the potential role of haptotaxis.

The TAF which diffuses from the tumour creates a chemical gradient. In this model, we assume that the EC secrete fibronectin in response to the TAF and hence move up an adhesive gradient of its own creation. Carter (1965) [4] suggested that a chemotactic substance may act indirectly by altering the surface of a cell and so increasing its adhesiveness. Fibronectin can bind to cell membranes by means of a specific fibronectin receptor thereby anchoring the cell to the ECM [26]. An adhesive gradient will be created as the surface nearest the chemical stimulus will be altered.

In the following section we develop a mathematical model for the initial formation of capillary sprouts, i.e. the budding process mentioned previously.

1.1 Mathematical Model

Let $n(\mathbf{x}, t)$ be the endothelial cell density and $c(\mathbf{x}, t)$ the concentration of fibronectin. We assume that there are only two contributions to cell flux at this stage —random motion and haptotaxis. Thus

$$\mathbf{J}_n = \mathbf{J}_{\text{diffusion}} + \mathbf{J}_{\text{haptotaxis}},$$

where in the usual way $\mathbf{J}_{\text{diffusion}} = -d_n(n)\nabla n$ and $\mathbf{J}_{\text{haptotaxis}} = a(c)n\nabla c$, and where d_n, a are the diffusion and haptotaxis coefficients respectively. For simplicity we will assume that these are constant. If N is the measure of the total number of cells and rN is the linear mitotic growth rate, then the net cell production can be modelled using a logistic-type growth rate and is given by $rn(N-n)$.

We assume that the fibronectin is simply secreted and diffuses into the surrounding area. The flux of the chemical fibronectin is given by $\mathbf{J}_c = -d_c\nabla c$, where d_c is the diffusion coefficient of the chemical again assumed to be constant. It is assumed that the production of fibronectin by the cells is given by the Michaelis-Menten production term $\dfrac{Sn}{(\beta + n)}$ and that the decay term is $-\gamma c$, where S, β, γ are positive constants.

Angiogenic activity is confined to a small region of the parent vessel wall nearest the tumour [25] . Initially, the vessel wall is simply a monolayer of EC. After the release of the TAF, some of the EC loosen their contacts with their neighbours and try to penetrate the basement membrane. Subsequently several EC follow the primary EC and pile up behind each other, creating a bulge in the wall of the capillary. Hence we need only consider the model in one spatial dimension in order to focus attention on clusters of cells rather than the overall shape of the buds. We assume that a region of increased cell density indicates the initiation of a cell cluster leading to a bud.

Conservation of mass gives us

$$n_t + \nabla.\mathbf{J}_n = f(n, c),$$

$$c_t + \nabla.\mathbf{J}_c = g(n, c).$$

where f, g contain appropriate source and sink terms. Hence the system of equations in one spatial dimension is

$$n_t = d_n n_{xx} - a(nc_x)_x + rn(N - n), \tag{1}$$

$$c_t = d_c c_{xx} + \frac{Sn}{(\beta + n)} - \gamma c. \tag{2}$$

During angiogenesis, EC in the parent vessel will actively move towards the tumour [1]. Experimental evidence shows that only a finite region of the parent vessel is involved in producing buds and hence we will take our spatial domain D to be finite. Given this geometry it is not unreasonable to treat the system as closed and impose zero flux boundary conditions.

$$d_n n_x - anc_x = 0\ ,\ c_x = 0 \ \text{ on } x \in \partial D,$$

$$\text{i.e. } n_x = c_x = 0 \text{ on } x \in \partial D.$$

We introduce dimensionless variables into the model in the following manner:

$$x^* = \left[\frac{\gamma}{d_c s}\right]^{\frac{1}{2}},\ t^* = \frac{\gamma t}{s},\ n^* = \frac{n}{\beta},\ c^* = \frac{\gamma c}{S},$$

$$N^* = \frac{N}{\beta},\ d^* = \frac{d_n}{d_c},\ a^* = \frac{aS}{\gamma d_c},\ r^* = \frac{r\beta}{\gamma},$$

where s is a scale factor with reference to the size of the domain. After non-dimensionalizing and dropping the asterisks for notational convenience, the equations become

$$n_t = dn_{xx} - a(nc_x)_x + srn(N-n), \tag{3}$$

$$c_t = c_{xx} + s\left[\frac{n}{n+1} - c\right], \tag{4}$$

$$n_x = c_x = 0,\ \ x = 0,\ 1. \tag{5}$$

We note that the above system of equations models the reaction of the EC to the TAF which is secreted by the tumour cells.

1.2 Linear Analysis

The spatially homogeneous steady states of the above system are given by

$$(n,c) = (0,0) \text{ and } (n,c) = (N, \frac{N}{N+1}).$$

The trivial state is not biologically relevant. We linearize about the non-trivial steady state in the usual manner by substituting

$$n = N + u \text{ and } c = \frac{N}{N+1} + v,$$

where $\mid u \mid, \mid v \mid$ are small, into the above equations to obtain the linearized system:

$$u_t = du_{xx} - aNv_{xx} - srNu, \tag{6}$$

$$v_t = v_{xx} + s\left[\frac{u}{(N+1)^2} - v\right]. \tag{7}$$

We look for solutions of the form $(u, v) \propto \exp(\sigma t + ikx)$. Hence we obtain the dispersion relation

$$\sigma^2 + \sigma[k^2(1+d) + s + srN] + k^2\left[d(k^2+s) + srN - \frac{saN}{(N+1)^2}\right] + s^2rN = 0. \tag{8}$$

The dispersion relation will have two roots and these will either be real or complex conjugates.

In the absence of any spatial variation the homogeneous steady state must be linearly stable, so that any instability will be diffusion driven. So by putting $k^2 = 0$ in the dispersion relation and solving for σ, we get

$$\sigma = -rNs, \ -s \leq 0.$$

So the spatially homogeneous steady state is linearly stable. We require $Re(\sigma(k^2)) > 0$

for instability. When $\sigma = 0$, we have

$$dk^4 + k^2 \left[ds + rNs - \frac{aNs}{(N+1)^2} \right] + rns^2 = 0.$$

$$k^2 = \frac{aNs - (ds + rNs)(N+1)^2}{2d(N+1)^2} \pm \frac{1}{2d} \left[\left(ds + rNs - \frac{aNs}{(N+1)^2} \right)^2 - 4drNs^2 \right]^{\frac{1}{2}}. \qquad (9)$$

Studies have shown that there is no significant increase in the rate of EC mitosis during the first stages of angiogenesis [1]. Mitosis occurs after the first sprouts have formed. It has been postulated that mitosis is a secondary reaction to angiogenesis resulting from abnormal permeability of the host vessels. Normal EC have a long half life and cell division is rare, occurring only when repair and remodelling of large wounds is essential [25]. It has also been shown that fibronectin inhibits cell proliferation to some extent [3]. We will consider the case where there is no mitosis and where there is mitosis at some background level separately.

1.2.1 No Mitosis (r=0)

Consider the case where there is no mitosis i.e. $r = 0$, then the system is similar to the model as examined in Myerscough and Murray (1992) [23] . Then from equation (9) we have

$$k^2 = \begin{cases} 0 \\ \dfrac{aNs}{d(N+1)^2} - s = k_2^2. \end{cases}$$

Hence the dispersion relation is tethered to the origin, which is expected when there is no proliferation of cells. By differentiating the dispersion relation with respect to k^2 and with $r = 0$ we obtain

$$\frac{d\sigma}{dk^2}(k^2(1+d)+s+2\sigma)+\sigma(1+d)+2dk^2+ds-\frac{saN}{(N+1)^2}=0.$$

Setting $\sigma = 0$,

$$\frac{d\sigma}{dk^2}=\frac{aNs}{(s+k^2(d+1))(N+1)^2}-\frac{ds+2dk^2}{s+k^2(d+1)}.$$

So, $\frac{d\sigma}{dk^2} > 0$ at the origin provided $\frac{aNs}{d(N+1)^2} - s > 0$, i.e. $k_2^2 > 0$. The maximum occurs at $\frac{d\sigma}{dk^2} = 0$, i.e. at k_M^2 where

$$\sigma_M(1+d)+2dk_M^2+ds-\frac{saN}{(N+1)^2}=0.$$

But if the maximum value is $\sigma = 0$ then $k_M^2 = 0$ as the dispersion relation is tethered to the origin as shown in figure (1). Hence $a_c = \frac{d(N+1)^2}{N}$ is the critical value of a. So provided $a > a_c$ we will have instability.

1.2.2 Mitosis included ($r > 0$)

In this model we will include some mitosis but at a reduced rate in order to account for the effect of fibronectin on the proliferation of EC [3]. Now consider $r > 0$. The critical value of k^2, k_c^2, occurs when equation (9) has only one root. i.e.

$$\left(ds+rNs-\frac{aNs}{(N+1)^2}\right)^2-4drNs^2=0, \tag{10}$$

$$k_c^2=\frac{1}{2d}\left(\frac{aNs}{(N+1)^2}-ds-rNs\right)=s\left(\frac{rN}{d}\right)^{\frac{1}{2}}. \tag{11}$$

So the critical value of a, a_c, is given by equation (10). A typical dispersion is shown in figure (2). Again when $a > a_c$ the system will be unstable. Also as $r \to 0$, $k_c^2 \to 0$ and $a_c \to \dfrac{d(N+1)^2}{N}$ which agrees with our earlier observations.

1.3 Estimation of parameters

Wherever possible experimental data was used to estimate the parameter values d, a, s, r and N. For simplicity we took S, $N = 1$.

Michaelis-Menten parameter β

We assume that the secretion of fibronectin by the EC is governed by Michaelis-Menten kinetics. Fibronectin molecules inside the EC form a complex by combining with receptors on the cell membrane. They are then carried across the membrane and deposited outside the cell. Upon derivation of the Michaelis-Menten term $\dfrac{Sn}{\beta+n}$, we observe that β represents the ratio between the rate at which the receptors become empty and the rate at which the receptors become occupied. Hence a reasonable estimate is $\beta = 1$.

Diffusion coefficient d

Sherratt and Murray (1990) [28] used estimated diffusion coefficients in their model of epidermal wound healing. For the diffusion of the cells they gave values of $3\times10^{-9}\text{cm}^2\text{s}^{-1}$, $3.5\times10^{-10}\text{cm}^2\text{s}^{-1}$ and $6.9\times10^{-11}\text{cm}^2\text{s}^{-1}$, and for the diffusion of the chemical in question they had $3.1\times10^{-7}\text{cm}^2\text{s}^{-1}$ and $5.9\times10^{-6}\text{cm}^2\text{s}^{-1}$. This gives a range for d of 9.6×10^{-1} to 1.2×10^{-5}. In their study of individual endothelial cells, Stokes et al. (1991) [31] calculated a random motility coefficient of $(7.1\pm2.7)\times10^{-9}\text{cm}^2\text{s}^{-1}$ for endothelial cells migrating in a culture containing an angiogenic factor αFGF [11], heparin and fetal calf serum. Taking

d_c as before, we obtain the range 1.4×10^{-2} to 7.5×10^{-4} for d. Hence we take $d = 10^{-3}$ in this case.

Rate of Mitosis r

For the rate of mitosis we took the range $0.04\mathrm{h}^{-1}$ (Sherratt and Murray (1990)) to $0.056\mathrm{h}^{-1}$ (Stokes and Lauffenburger (1991) [30]). However according to Bowersox and Sorgente (1982) [3] , fibronectin inhibits cell proliferation by 23% . Hence we have a range of $0.0308\mathrm{h}^{-1}$ to $0.043\mathrm{h}^{-1}$ for cell mitosis. Yamada and Olden (1978) reported on the turnover rate of cell surface fibronectin. Fibronectin has a generation time of 18 hours with half remaining after 36 hours. This gives a half life of 18 hours and so the rate of decay is given by $\gamma = \frac{1}{18} ln 2 \simeq 0.0385 h^{-1}$. Hence we took $r = \frac{0.034}{0.0385} \simeq 0.88$.

Haptotaxis coefficient a

The Boyden chamber can be used to evaluate cell migration. Using this method, Ungari et al. (1985) [33] found that fibronectin mobilized EC at a dose between $5\mu g/\mathrm{ml}$ to $20\mu g/\mathrm{ml}$. Bowersox and Sorgente (1982) found that the maximum response by EC was at $100\mu\mathrm{g/ml}$ and Terranova et al. (1985) [32] found that doses of fibronectin between $10^{-8}\mathrm{M}$ and $10^{-10}\mathrm{M}$ stimulated cell migration. However, this method fails to give information about the haptotaxis coefficient. Therefore we ran several numerical simulations and found that the best results were obtained with a value of $a = 3.8$. Hence, using the values of γ and d_c which we found previously, we obtain a haptotaxis coefficient of $1.46 \times 10^{-7}\mathrm{cm}^2\mathrm{s}^{-1}\mathrm{M}^{-1}$.

Size of domain s

The parameter value s represents the finite region of the capillary vessel that is affected by the TAF. s will depend on the distance between the tumour and the capillary. As a scale reference, we will take $s = 1$ when the tumour is at a maximum distance from the capillary but still close enough for angiogenesis to take place.. From the summary of corneal implants as reported in Balding and McElwain (1984) [2], the distance between the tumour and the host vessel should be in the range 0.8mm to 2.5mm in order to achieve neovascularization. Gimbrone et al. (1974) [12] observed that capillary sprouts did not grow until the tumour implant was placed within 2.5±0.5mm from the limbal vessels. Therefore we can take our domain size s to be in the range 1 to 3. By increasing the size of the domain we can obtain a larger variety of pattern. Hence, we will take $s = 3$.

1.4 Numerical Results

The non-dimensionalized system of equations was solved using a routine available from the NAG library which integrates parabolic partial differential equations via the method of lines and Gear's method. The parameter values used were as specified in the previous section and we had zero flux boundary conditions. As predicted by the linear analysis the system evolved into a spatially inhomogeneous solution (see figures (3) and (4)). The peaks in the cell density shows that the cells have moved from their evenly distributed positions and have clustered together to form buds. These buds will sprout towards the tumour and will become the primary capillary vessels in the vasculature of the tumour. Our simulation shows that two clusters form initially, an observation made by Muthukkaruppan et al. (1982) in their experiments with mouse cornea. The distribution of the chemical fibronectin and the distribution of the cells are similar. Thus the cells have moved towards areas of high chemical concentration. As fibronectin is associated with cell adhesion, we conclude that the mechanism by which the cells move is via haptotaxis. The maxima in the chemical concentration coincide with the intensity of the TAF diffusing from the tumour i.e. the point of initial contact between the parent vessel and the TAF is the area where the first sprouts will be observed.

This model illustrates the principle of local activation and lateral inhibition [24] . Once a peak in fibronectin concentration has been established, EC will actively move up the adhesive gradient and hence the concentration of chemical in that area will increase. Even more cells will move into that particular area and so on. Zones of inhibition will be created as cells move away from areas of low chemical concentration. These are indicated by the minima in figures (3) and (4). This highlights the importance of domain size to pattern formation. If the domain was too small, the cells would become saturated with fibronectin and would not be able to detect gradients in the chemical/adhesive sites. Hence the zones of inhibition would disappear and so would the pattern.

In the next section we will focus upon EC within the capillary sprout in order to investigate the branching process and the involvement of haptotaxis.

2 The Branching of Capillary Sprouts

We now consider events after the formation of capillary buds. Having broken through the basement membrane, the buds will elongate and form sprouts by recruiting EC from the parent vessel. As the sprouts grow towards the tumour, secondary side branching will occur, whereby the sprouts themselves bud in a similar manner to those which developed from the parent vessel.

There are two separate processes involved in the creation of branching structures such as trees, corals and bryozoans.

1. The growth of branches.

2. The splitting of one branch into two.

As the resultant patterns depend upon the timing and the location of a splitting branch, there are often significant differences between branching structures so that each one is distinct. Balding and McElwain (1985) observed several similarities between fungal growth and neovascularization and subsequently based their model for capillary growth on the model of fungal colonies by Edelstein (1982) [7].

Similar structures are known to arise during the growth and development of bryozoans. Growth in bryozoans occurs at the tips of the branches. Cells lying inside a growing tip secrete the cuticle as the branch grows. The new cuticle is inserted directly into the existing cuticle, which spreads out carrying cells and adhesive sites with it. The older cuticle is pushed outwards and calcifies forming the outer layer of the branch. The direction of branch growth depends upon the location of the cells within the tip and the splitting of a cell cluster into two coincides with the splitting of one branch into two. Hence the splitting of a cell cluster is the initial event which determines branching.

The model of bryozoan growth proposed by Goldwasser et al. (1989) [13] may be adapted to describe other branching structures. In particular it could be used as the basis for a model mechanism describing the branching of capillary sprouts during angiogenesis. The growing capillary sprout tip is analogous to the growing tip of a bryozoan in that branching occurs when a cell cluster splits into two. From experimental observations we can assume that during angiogenesis the EC secrete a matrix consisting of fibronectin, laminin and collagen IV [25] and the movement of the EC is determined by the distribution of adhesive sites on this matrix. We can attribute the loss of matrix to the reformation of a basement membrane during the maturation of the newly formed sprouts. It is known that convection plays a major role in the transport of tissue [21]. We also know that EC move up and down the new capillary [25] and this cannot be explained either by directed cell motion alone, such as chemotaxis, or by random motility. Thus, we can assume that the matrix spreads out and the that the EC are to some extent passively carried with it. As proliferation occurs at some distance from the tip of the capillary sprout [1], [25] we do not need to include mitosis in the model.

2.1 Mathematical Model

The model is constructed in a one-dimensional domain in order to focus attention on the cell clusters, rather than the emerging shape of the branch tip. Let $r(x,t)$ be the density of the matrix (or cuticle), $a(x,t)$ the density of the adhesive sites and $n(x,t)$ the density of the cells at each point x at time t.

Many models of tumour angiogenesis rely on chemotaxis as a mechanism for cell motion. However chemotaxis is insufficient to account for all events. Chemotaxis is implicit in this model, that is all the events of angiogenesis occur after the release of TAF by the tumour. Cells at the tips of the sprouts react to the chemotactic stimulus through migration and proliferation. It is these cells at the tips which primarily orientate the direction of the sprouts. We focus attention on EC behind the proliferating cells and hence it can be assumed, based on experimental evidence cited previously, that the movement of the EC (within the region of the sprout under consideration) in this case is governed by a combination of diffusion, haptotaxis and convection.

The model is based on two processes.

1. The spreading of the matrix with the convection of cells and adhesive sites with it.

2. The secretion of matrix and adhesive sites by the cells.

The convection of cells and adhesive sites will be at the same rate at which the matrix spreads out. Assuming that the matrix spreads out at a constant rate, c say, and that the velocity is $-r_x$, then the convective flux is proportional to $-cr_x$, i.e. flux of the matrix is $J_r = -crr_x$. For the source and sink terms, we assume exponential production and decay of the matrix and adhesive sites, but as proliferation of EC occurs at some distance from the tip, we omit a cell production term. Hence the model equations are,

$$r_t = d_1 r_{xx} + c(rr_x)_x + \zeta n - \lambda r, \tag{12}$$

$$a_t = d_2 a_{xx} + c(ar_x)_x + bn - \mu a, \tag{13}$$

$$n_t = d_3 n_{xx} - h(na_x)_x + c(nr_x)_x. \tag{14}$$

c is the rate at which the matrix spreads.

ζ is the rate of secretion of matrix per cell.

λ is the loss of matrix per unit matrix.

b is the rate of secretion of adhesive sites per cell.

μ is the decay of adhesive sites.

d_1, d_2, d_3 are the diffusion constants.

h is the rate at which cells move up an adhesive gradient.

2.2 Non-Dimensionalization

Let N be the mean endothelial cell density throughout the domain, L_0 the original length of the domain, i.e. the length of the initial sprout bud and L the current length. The above system of equations can be non-dimensionalized by making the following substitutions:

$$n^\star = \frac{n}{N},\ x^\star = \frac{x}{L},\ t^\star = \frac{\mu L_0^2 t}{L^2},\ a^\star = \frac{ah}{\mu L_0^2},\ r^\star = \frac{rc}{\mu L_0^2},$$

$$\lambda^\star = \frac{\lambda}{\mu},\ \gamma^\star = \frac{L^2}{L_0^2},\ \zeta^\star = \frac{cN\zeta}{\mu^2 L_0^2},\ b^\star = \frac{bhN}{\mu^2 L_0^2},\ d_i^\star = \frac{d_i}{\mu L_0^2},\ i = 1, 2, 3.$$

Dropping the asterisks for notational convenience, the system of equations become,

$$r_t = d_1 r_{xx} + (r r_x)_x + \gamma(\zeta n - \lambda r), \tag{15}$$

$$a_t = d_2 a_{xx} + (a r_x)_x + \gamma(bn - a), \tag{16}$$

$$n_t = d_3 n_{xx} - (n a_x)_x + (n r_x)_x. \tag{17}$$

To close the system we impose non-zero flux boundary conditions for the matrix and the adhesive sites, but zero flux boundary conditions for the cells.

2.3 Linear Analysis

Assuming that the number of cells in the domain remains constant, i.e. no proliferation in the region that we are considering, then n=1. The non-trivial spatially homogeneous steady state is ($\frac{\zeta}{\lambda}$, b, 1). After linearizing about this steady state , we look for solutions of the form

$$\begin{bmatrix} r - \dfrac{\zeta}{\lambda} \\ a - b \\ n - 1 \end{bmatrix} \propto \exp(\sigma t + ikx),$$

where k is the wave number of the perturbation and σ is the rate of growth of the perturbation with wave number k.

The linearized system of equations takes the form $\sigma\mathbf{r} = A\mathbf{r}$ where A is a 3×3 matrix and $\mathbf{r} = [\overline{\mathbf{r}},\ \overline{\mathbf{a}},\ \overline{\mathbf{n}}]^{\mathbf{t}}$.

The dispersion relation between σ and k is given by $\det[\sigma I - a] = 0$ and is shown below.

$$\begin{aligned} \sigma^3 &+ \sigma^2[k^2(d_1 + d_2 + d_3 + \frac{\zeta}{\lambda}) + \gamma(\lambda+1)] \\ &+ \sigma[k^2\gamma(d_1 + \lambda d_2 + (1+\lambda)d_3 - b + \frac{\zeta}{\lambda} + \zeta) + k^4(d_2 + d_3)(\frac{\zeta}{\lambda} + d_1) + \gamma^2\lambda] \\ &+ k^2[\gamma^2(\lambda(d_3 - b) + \zeta) + k^2\gamma((d_3 - b)(\frac{\zeta}{\lambda} + d_1) + \zeta(b + d_2) + d_2 d_3\lambda) \\ &+ k^4 d_2 d_3(\frac{\zeta}{\lambda} + d_1)] = 0. \end{aligned} \tag{18}$$

If $\mathrm{Re}(\sigma) < 0$ then $\exp(\sigma t + ikx) \to 0$ as $t \to \infty$, so the system will be stable. If $\mathrm{Re}(\sigma) > 0$ the perturbations will grow. The imaginary part of σ gives rise to periodic solutions. When $k = 0$, i.e. the system is spatially homogeneous, the dispersion relation becomes

$$\sigma^3 + \gamma(\lambda+1)\sigma^2 + \gamma^2\lambda\sigma = 0, \tag{19}$$

which has the solution $\sigma = 0$ and two negative roots. Hence the system is stable to spatially homogeneous solutions. When $k \neq 0$ the dispersion relation will either have three real roots or one real root and two complex conjugate roots. The root whose real part is the greatest will determine the pattern formation. If this root is real and positive for a range of k, the initially uniform cell distribution will evolve into a spatially heterogeneous one. If this root is complex and its real part is positive then the perturbation will be oscillatory.

We will have a change in stability when $\sigma = 0$, i.e. $p(k^2) = 0$ where

$$p(k^2) = a_1 k^4 + a_2 k^2 + a_3,$$

and

$$a_1 = d_2 d_3 \left(\frac{\zeta}{\lambda} + d_1 \right),$$

$$a_2 = \gamma \left((d_3 - b)(\frac{\zeta}{\lambda} + d_1) + \zeta(b + d_2) + d_2 d_3 \lambda \right),$$

$$a_3 = \gamma^2 (\zeta + \lambda(d_3 - b)).$$

If $a_2 > 0$ and $a_3 > 0$, then $p(k^2)$ has no positive solutions for k^2. Now consider the case where $a_3 < 0$. In this case $p(k^2)$ has one positive root. So if $b > d_3 + \frac{\zeta}{\lambda}$, then we have stability for $0 < k^2 < k_c^2$ where k_c^2 is the positive root of $p(k^2)$. If $a_3 > 0$ but $a_2 < 0$, then $p(k^2)$ has two positive roots, i.e. if $b < d_3 + \frac{\zeta}{\lambda}$ and

$$b(\frac{\zeta}{\lambda} + d_1 - \zeta) > d_3(\frac{\zeta}{\lambda} + d_1) + d_2 \zeta + d_2 d_3 \lambda,$$

then we have instability for $k_A^2 < k^2 < k_B^2$ where $k_{A,B}^2$ are the roots of $p(k^2)$.

Returning to the dispersion relation, we now consider the signs of the coefficients of the cubic equation (18), i.e. the signs of

$$A_1 = k^2(d_1 + d_2 + d_3 + \frac{\zeta}{\lambda}) + \gamma(\lambda + 1),$$

$$A_2 = k^2\gamma(d_1 + \lambda d_2 + (1+\lambda)d_3 - b + \frac{\zeta}{\lambda} + \zeta) + k^4(d_2 + d_3)(\frac{\zeta}{\lambda} + d_1) + \gamma^2\lambda,$$

$$A_3 = k^2(\gamma^2(\lambda(d_3 - b) + \zeta) + k^2\gamma((d_3 - b)(\frac{\zeta}{\lambda} + d_1) + \zeta(b + d_2) + d_2 d_3\lambda) + k^4 d_2 d_3(\frac{\zeta}{\lambda} + d_1)).$$

Since $A_1 > 0$ for all positive parameters, if $A_3 < 0$ then (18) has only one positive root which will be real. If $A_3 > 0$ and $A_2 > 0$, the dispersion relation will have no positive roots. However if $A_3 > 0$ and $A_2 < 0$ then the dispersion relation has two positive roots. So consider $q(k^2) = 0$ where $q(k^2) = b_1 k^4 + b_2 k^2 + b_3$ and

$$b_1 = (d_2 + d_3)(\frac{\zeta}{\lambda} + d_1),$$

$$b_2 = \gamma(d_1 + \lambda d_2 + (1+\lambda)d_3 - b + \frac{\zeta}{\lambda} + \zeta).$$

$$b_3 = \lambda\gamma^2.$$

If $b_2 > 0$ then $q(k^2)$ has no positive roots. If $b_2 < 0$ then $q(k^2)$ has two positive roots. So for $k_2^2 < k^2 < k_1^2$, where $k_{1,2}^2$ are the roots of $q(k^2)$, i.e for

$$b > d_1 + \lambda d_2 + (1+\lambda)d_3 + \frac{\zeta}{\lambda} + \zeta,$$

the dispersion relation has two positive roots and hence we have instability.

There exists another bifurcation point at which two of the real roots become complex.

This point k_b^2 say, is given by solving

$$|\beta| = 2\alpha^{3/2}$$

for k^2 where

$$\alpha = \left(\frac{A_1}{3}\right)^2 - \left(\frac{A_2}{3}\right), \quad \beta = 2\left(\frac{A_1}{3}\right)^2 - \left(\frac{A_1 A_2}{3}\right) + A_3.$$

A summary of the changes in the roots of the dispersion relation as k^2 increases is as follows.

- For $0 < k^2 < k_c^2$ the dispersion relation has one positive and two negative real roots.
- For $k_c^2 < k^2 < k_b^2$ all the roots are real and negative.
- For $k_b^2 < k^2 < k_2^2$ all roots are negative but two roots are complex and one root is real.
- For $k_2^2 < k^2 < k_1^2$ the dispersion relation has one negative real root and two positive complex roots.
- For $k_2^2 < k^2$ all roots are negative.

Consider the case where $d_1 = d_2 = 0$. In this case we will have exponential growth provided

$$k^2\gamma^2(\lambda d_3 - b\lambda + \zeta) + k^4\gamma\zeta(\frac{d_3 - b}{\lambda} + b) < 0,$$

(see Murray (1989) [21]). Thus for k^2 in the range

$$0 < k^2 < \gamma(\lambda(b - d_3) - \zeta)/\zeta(\frac{d_3 - b}{\lambda} + b) = k_c^2$$

growth will be exponential. The limiting case is where $k_c^2 = 0$. Then the critical value of the parameter b, b_c say, is given by $b_c = d_3 + \frac{\zeta}{\lambda}$. So when $b > b_c$ we will have instability. For example, by using the parameters $d_1 = 0,\ d_2 = 0,\ d_3 = 10,\ b = 169,\ \lambda = 20,\ \gamma = 13, \zeta = 10$, we obtain the dispersion relation as shown in figure (5). So for $0 < k^2 < 5.0585$, we will have exponential growth.

Another example is if we use the parameters $d_1 = 1,\ d_2 = 1,\ d_3 = 10,\ b = 250,\ \lambda = 20,\ \gamma = 12,\ \zeta = 10$. For these parameters we obtain the dispersion relation as shown in figure (6) where two of the roots of the dispersion relation have become complex and positive. In this case we would expect oscillating solutions.

2.4 Estimation of parameters

Wherever possible parameters were estimated from experimental papers. When this proved difficult, the parameters were chosen in order to give the best numerical results.

From Balding and McElwain (1985) and Gimbrone et al. (1974), the tumour must be placed at a distance of 0.08–0.3cm from the limbal vessel. Hence, we will take the initial length $L_0 = 0.001$cm and let L vary between 0.003–0.011cm so that $9 < \gamma < 121$.

Using the results from Yamada and Olden (1978), we estimate the decay of the matrix to be 0.0385h^{-1}. If we take $\lambda = 20$ then the decay of the adhesive sites μ is $1.925 \times 10^{-3}\text{h}^{-1}$. The choice of λ was arbitrary due to the lack of empirical data.

Yamada and Olden (1978) reported that fibronectin is relatively immobile with diffusion coefficient $< 5 \times 10^{-12}$. So taking the diffusion of the matrix and the diffusion of the adhesive sites to be $5.35 \times 10^{-13}\text{cm}^2\text{s}^{-1}$ and the diffusion of the cells to be ten times higher, we have $d_1 = d_2 = 1$ and $d_3 = 10$. By making the diffusion of the cells lower than expected, we will emphasize the other transport mechanisms.

Terranova et al. (1985) found that doses of fibronectin between $10^{-8} - -10^{-10}$M stimulated cell migration and Yamada and Olden (1978) gave the generation time of fibronectin to be 18 hours. Assuming that 10^{-8}M of fibronectin is produced by N cells in 18 hours, where N is the mean cell density, we estimate the rate of the secretion of the matrix as $\frac{10^{-8}}{18}N^{-1}\text{h}^{-1}\text{M}$. Again choosing ζ arbitrarily to be 10, we find that $c = 1.854738 \times 10^{-5}\text{cm}^2\text{s}^{-1}\text{M}^{-1}$, which seems a reasonable estimate for the convection rate. Assuming that the secretion of the adhesive sites is ten times higher than that of the matrix and choosing $b = 250$ and $b = 169$, we obtain $h = 4.636845 \times 10^{-5}\text{cm}^2\text{s}^{-1}\text{M}^{-1}$ and $h = 3.345 \times 10^{-5}\text{cm}^2\text{s}^{-1}\text{M}^{-1}$.

2.5 Numerical Analysis

NAG routine D03PGF was used to solve the non-dimensionalized system of equations. (This NAG routine integrates via the method of lines and Gear's method.) We impose non–zero flux boundary conditions for the matrix and the adhesive sites, but zero flux boundary conditions for the cells. This seems reasonable as we are only considering the splitting of a cell cluster rather than the actual formation and elongation of the branches. To model the formation of the branches themselves we would need to have a moving domain.

The boundary conditions were taken to be

$$\begin{aligned} rr_x &= \mp k, \\ ar_x &= \mp l, \\ dn_x - na_x &+ nr_x = 0. \end{aligned} \tag{20}$$

at x=0 and x=1 respectively where k and l are positive constants.

By using the parameter values $d_1 = 1,\ d_2 = 1,\ d_3 = 10,\ b = 250,\ \lambda = 20,\ \gamma = 12,\ \zeta = 10$ we would expect oscillatory solutions. A qualitative result is obtained whereby peaks in the concentration of cells form from the initial conditions and move towards each other eventually merging and then splitting again. (figures (7), (8)), (9)), (10)), (11)), (12)), (13)) and (14)).

Goldwasser et al. (1989) obtain the result where one cell cluster forms when $k_m = \pi$ and two cell clusters when $k_m = 2\pi$, k_m being the fastest growing wavenumber. By using the parameter values $d_1 = 0,\ d_2 = 0,\ d_3 = 10,\ b = 169,\ \lambda = 20,\ \gamma = 13,\ \zeta = 10$ in the above NAG routine we obtain the top picture in figures (15), (16)) and (17)) where the density of the cells is greater at one end of the domain indicating the formation of one cell cluster. We can increase the number of cell clusters formed by increasing our value of γ, which is representative of the size of the domain, i.e $\gamma \propto k^2$. So for two cell clusters we take $\gamma_2 = 4\gamma$, for three cell clusters take $\gamma_3 = 9\gamma$ and so on. Hence as the domain increases the more branches there are.

2.6 Discussion

The models for capillary bud and capillary branch formation were developed using empirical data wherever possible and the numerical solutions of the models are in good agreement with experimental observations of tumour angiogenesis.

It is our belief that the events of angiogenesis cannot be fully explained by chemotaxis alone. We have shown that haptotaxis is an important mechanism throughout all stages of angiogenesis and is worthy of further study. Schor and Schor (1983) [27] found that components of the ECM, such as fibronectin, increased the ability of EC to react to angiogenic factors positively. Furthermore, they discovered that EC did not react to an angiogenic stimulus when grown on denatured collagen or plastic material. Haptotaxis has been implicated in the formation of anastomoses [25]. Though this important event in angiogenesis is rarely studied, it is known that capillary sprouts fuse together at their tips. This indicates that some mechanism which induces cell to cell adhesion must be involved.

The models that we have considered are minimal in that they include the most basic of equations concerning the chemical and cell distribution. We can elaborate the models to include other factors such as the effect of traction forces on the matrix (see for example [20]). It may be possible to gain some useful information on lumen formation and anastomosis by producing two dimensional simulations of these models. We could also consider non-constant diffusion/haptotactic coefficients. Nevertheless, these simple models have produced the desired results by encapsulating the formation of capillary buds and the branching of capillary sprouts.

List of Figures

Figure (15)–Figure (17): By increasing our value of γ the number of cell clusters formed increases. Parameter values are $d_1 = 0,\ d_2 = 0,\ d_3 = 10,\ b = 169,\ \lambda = 20,\ \zeta = 10,\ \gamma = 13,\ 52,\ 108$.

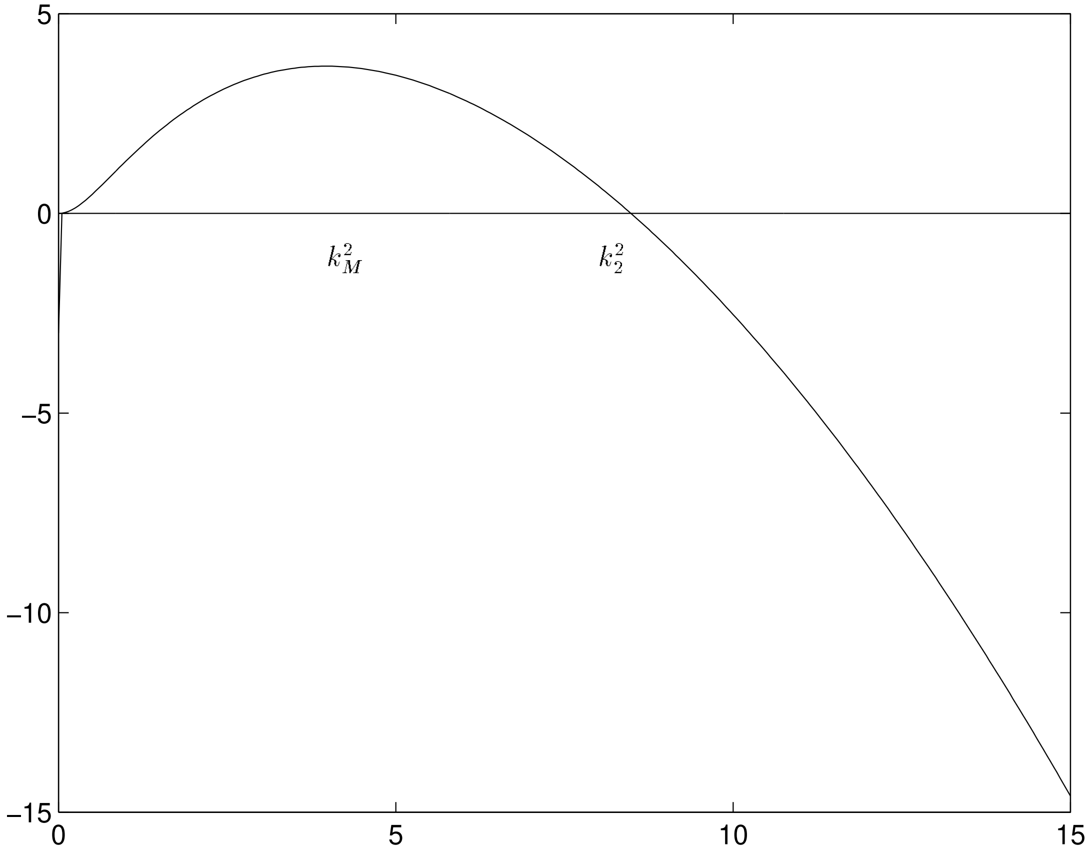

Figure 1:

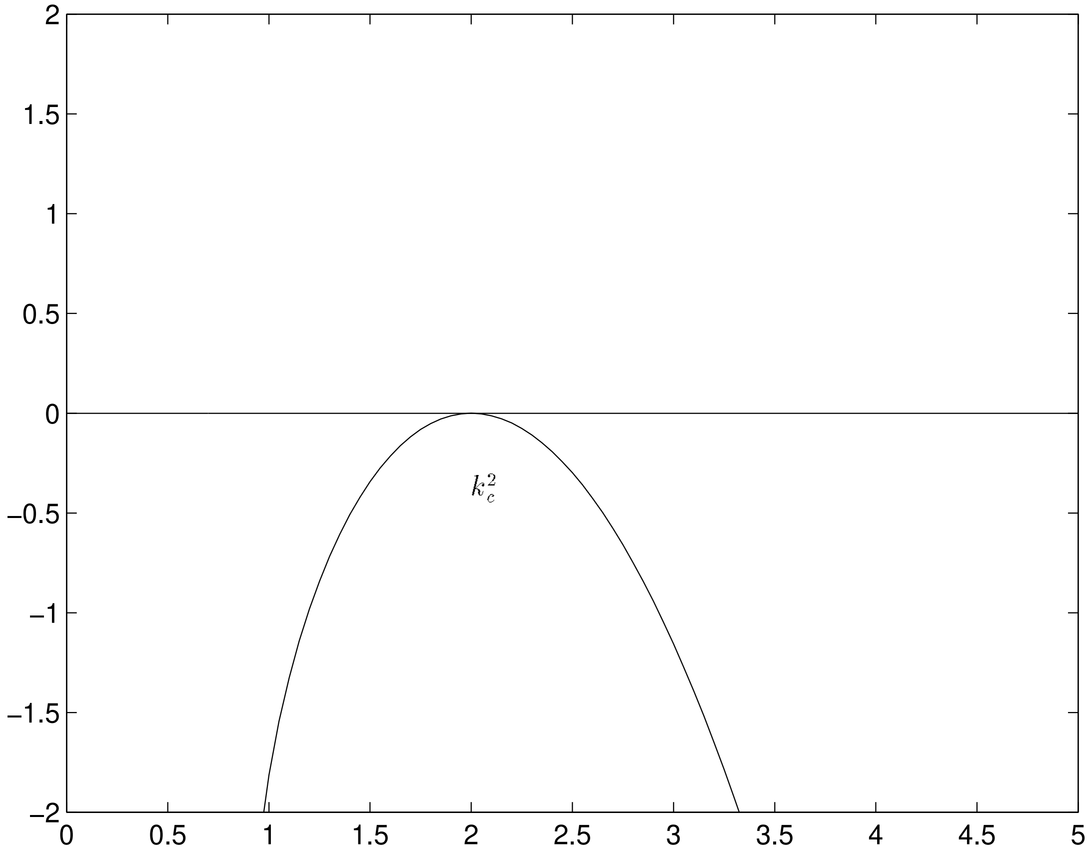

Figure 2:

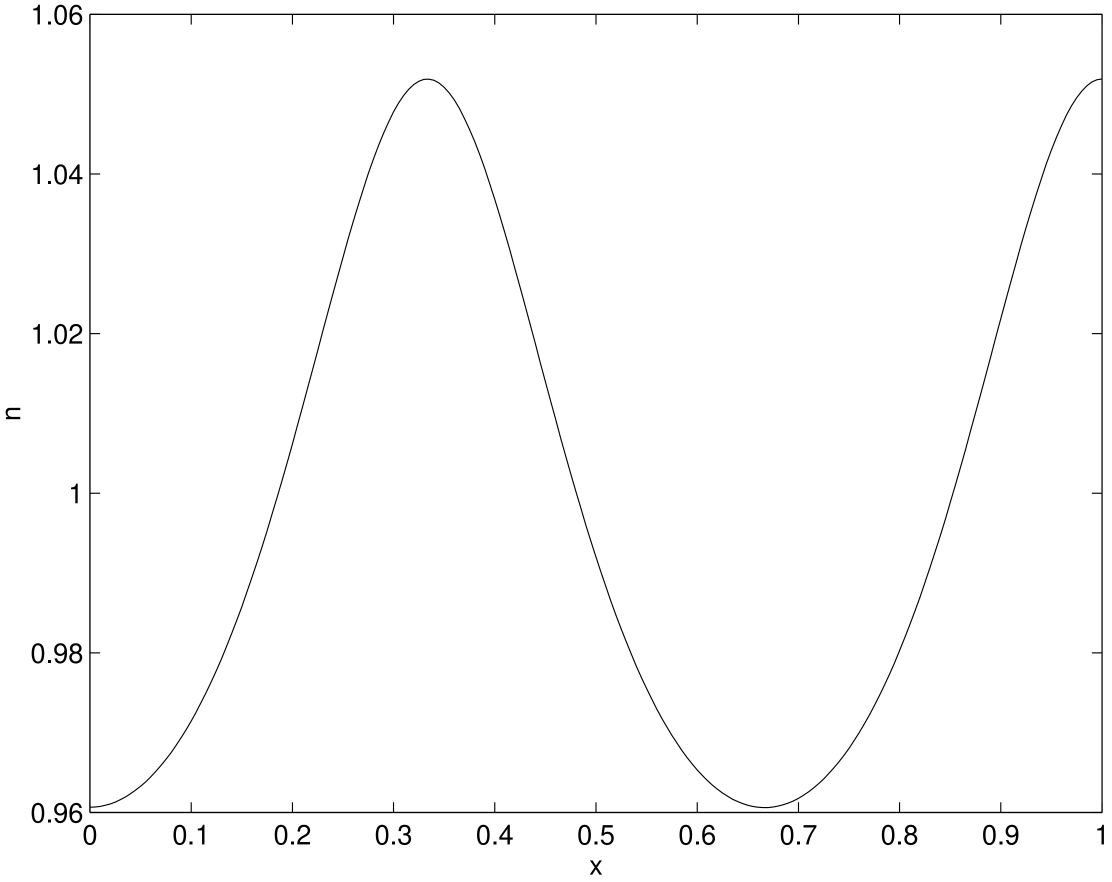

Figure 3:

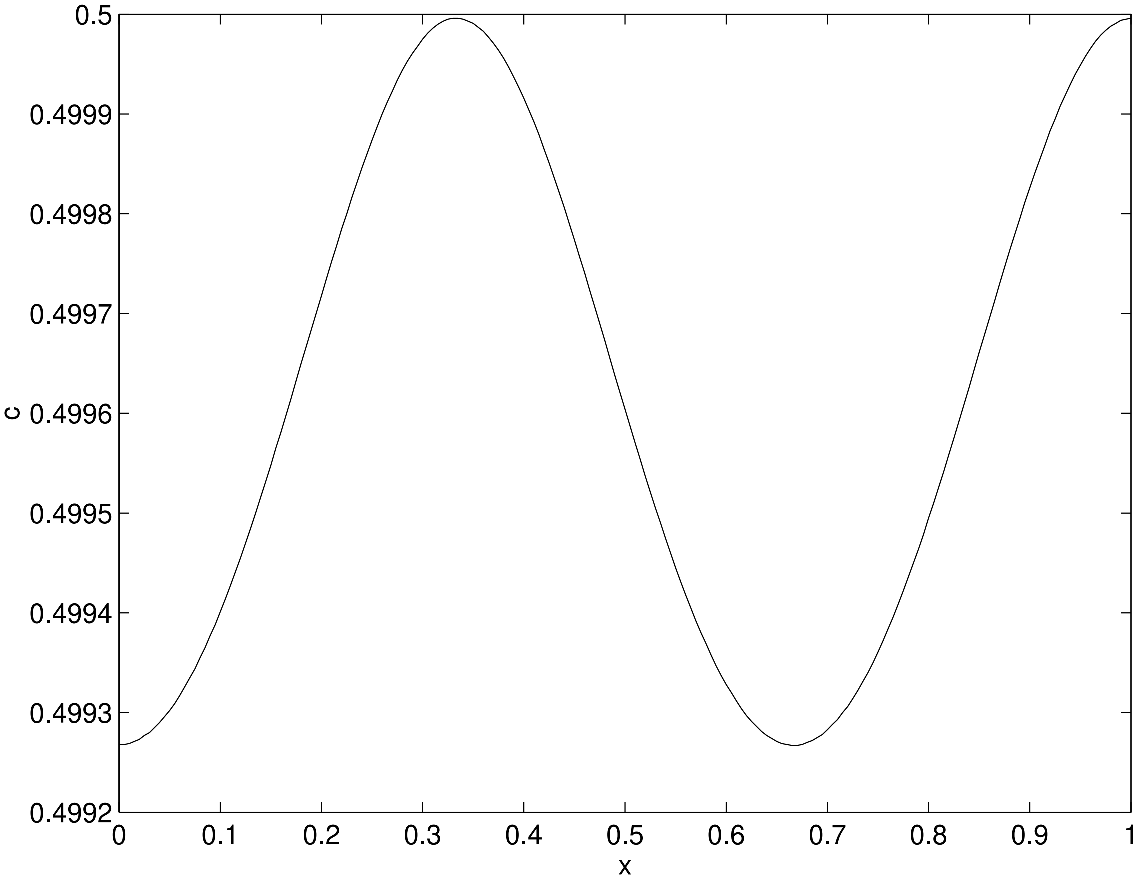
0.5
0.4999
0.4998
0.4997
0.4996
0.4995
0.4994
0.4993
0.4992
c
0
0.1
0.2
0.3
0.4
0.5
0.6
0.7
0.8
0.9
1
x

Figure 4:

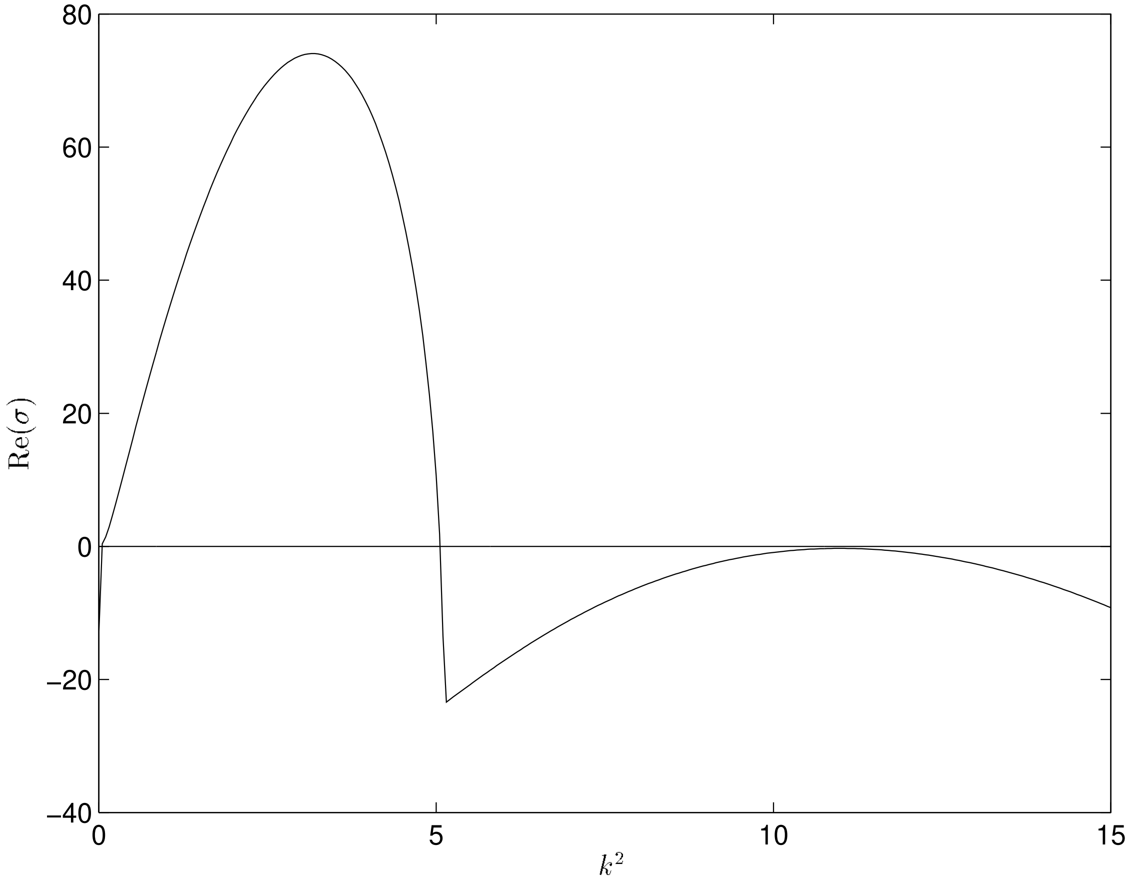

Figure 5:

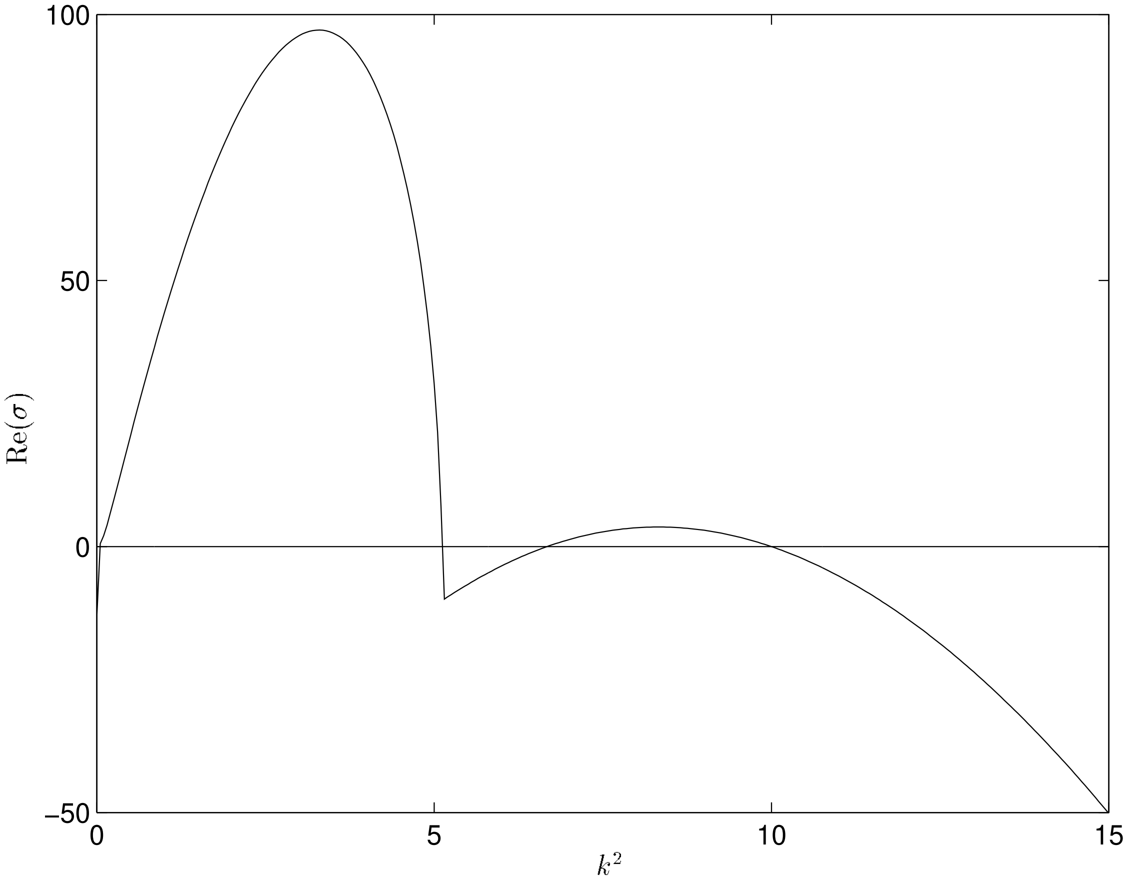

Figure 6:

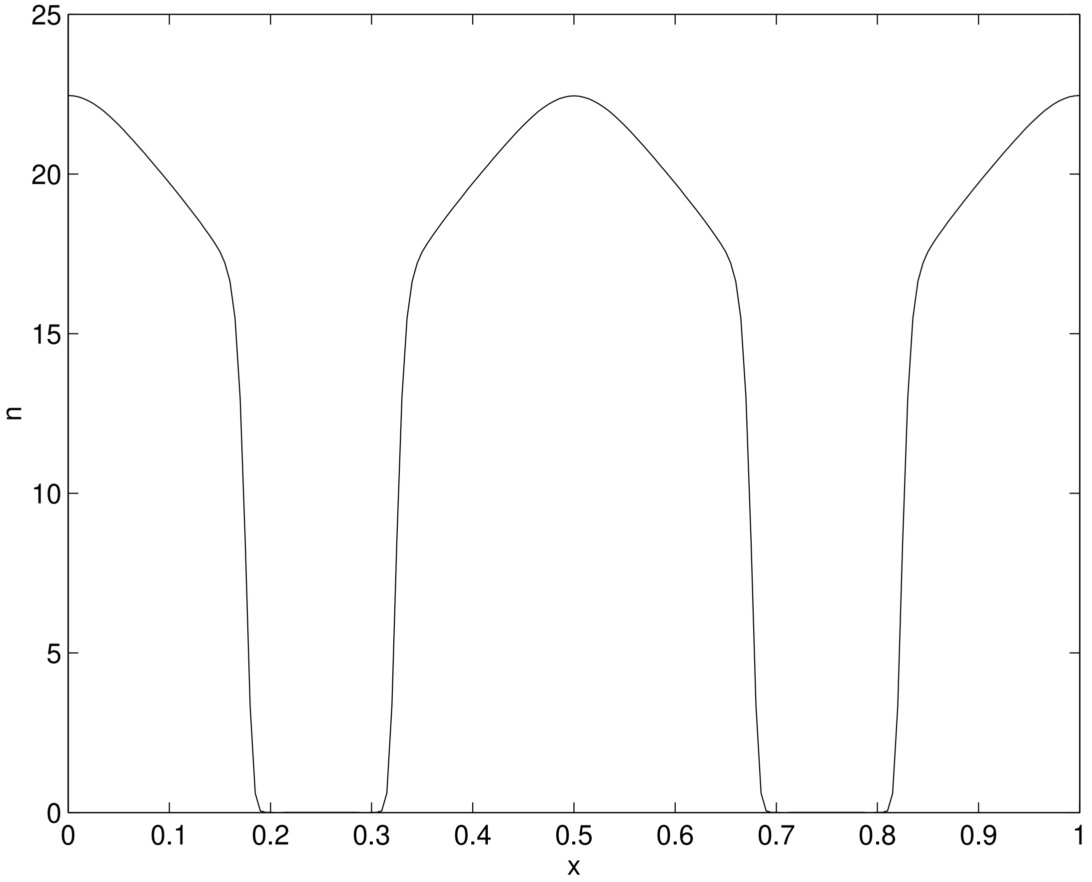

Figure 7:

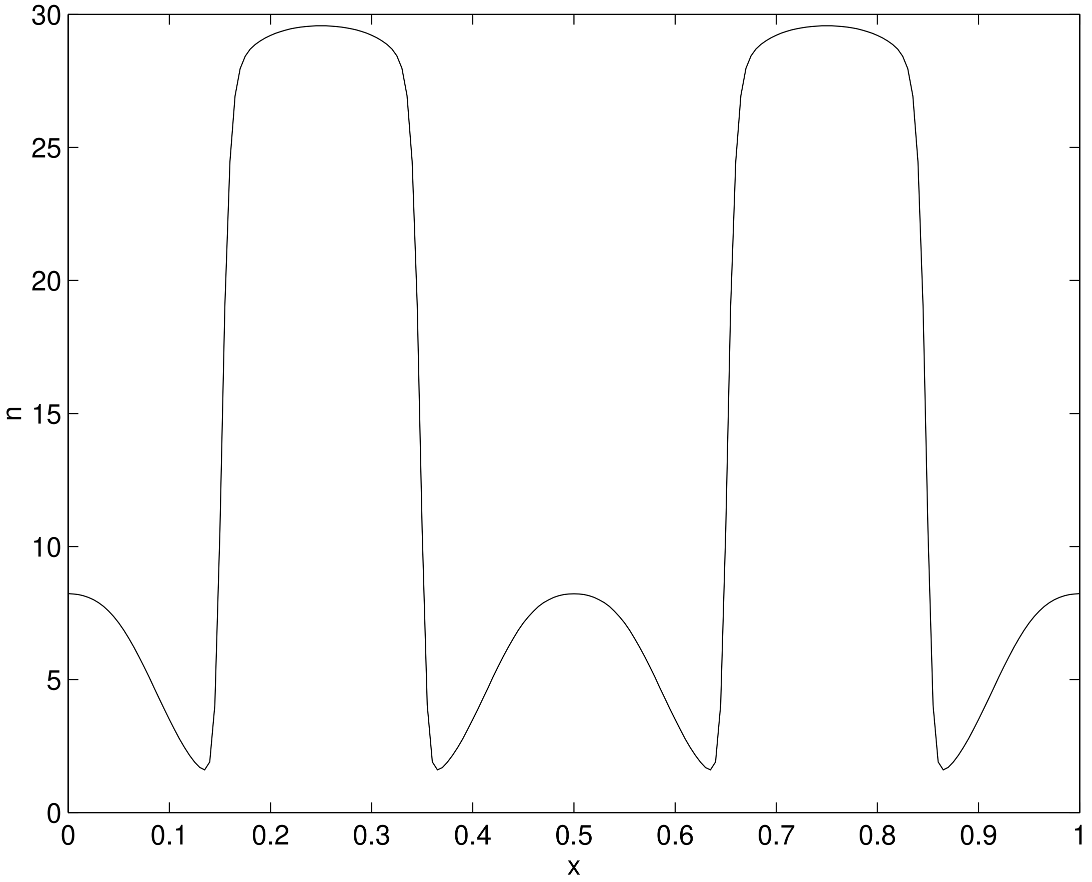

Figure 8:

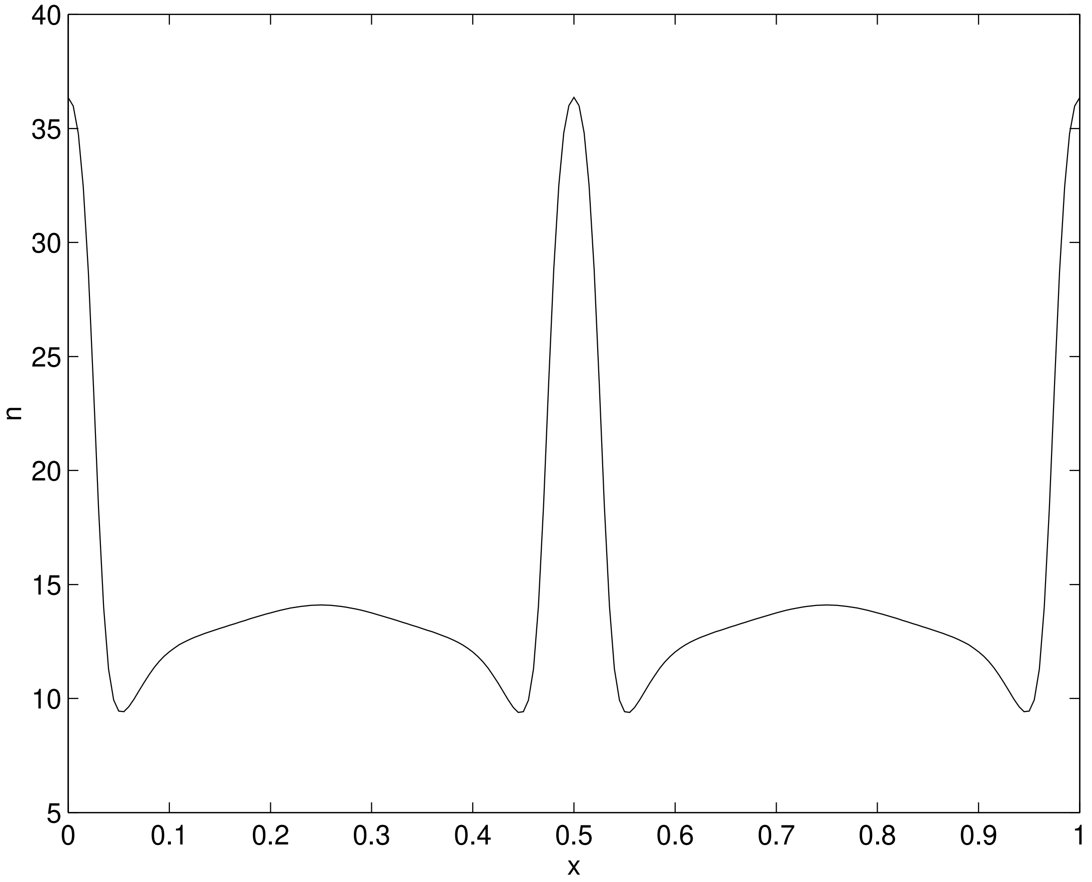

Figure 9:

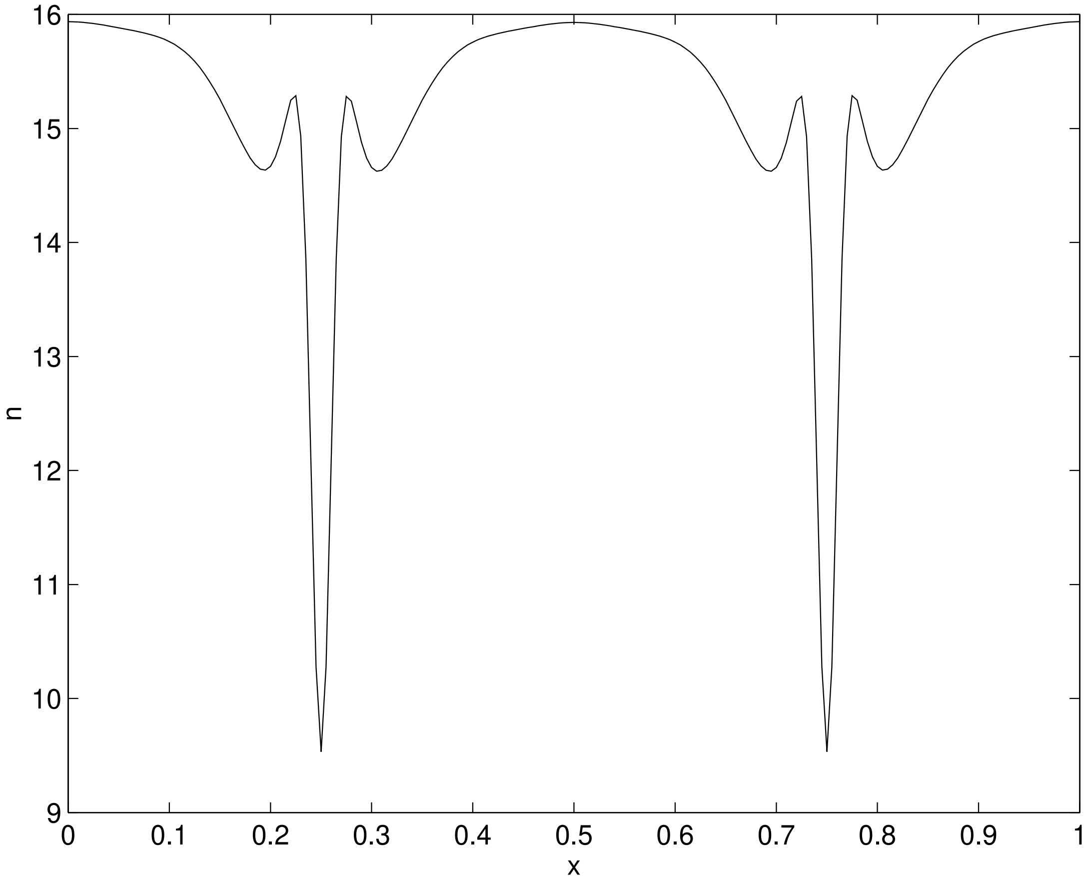

Figure 10:

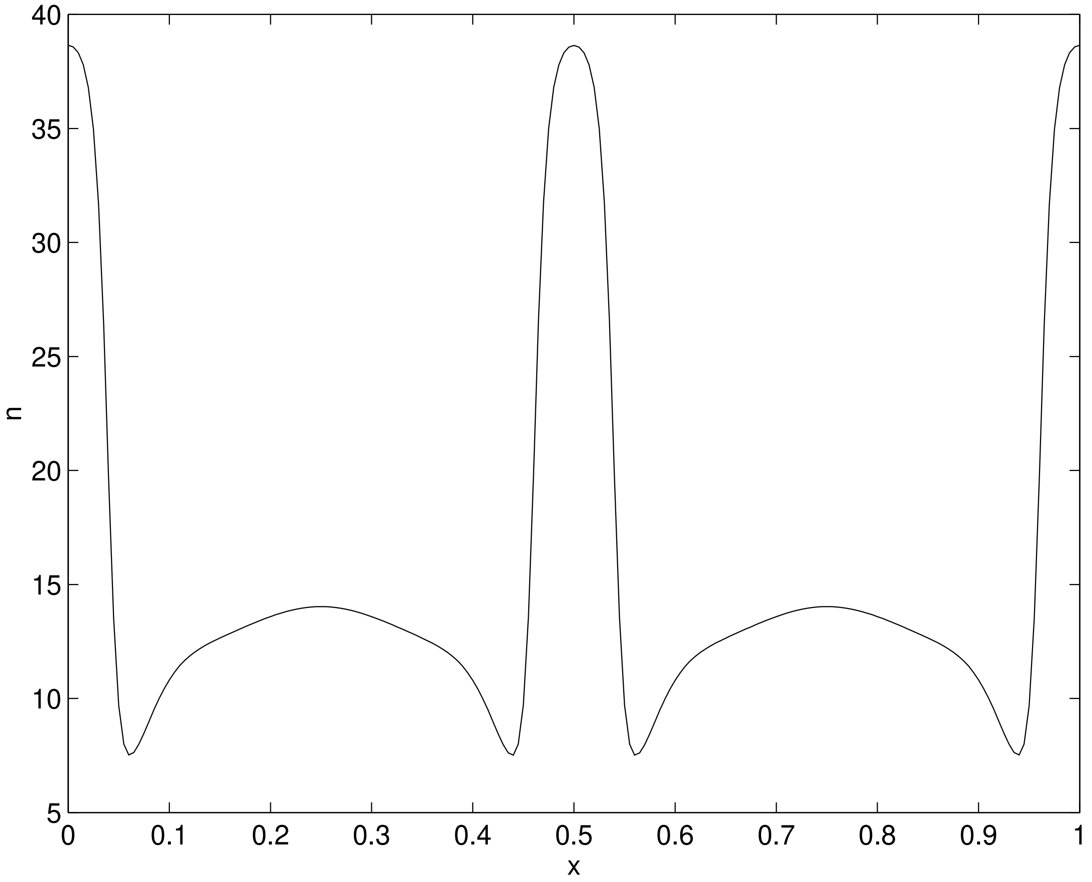

Figure 11:

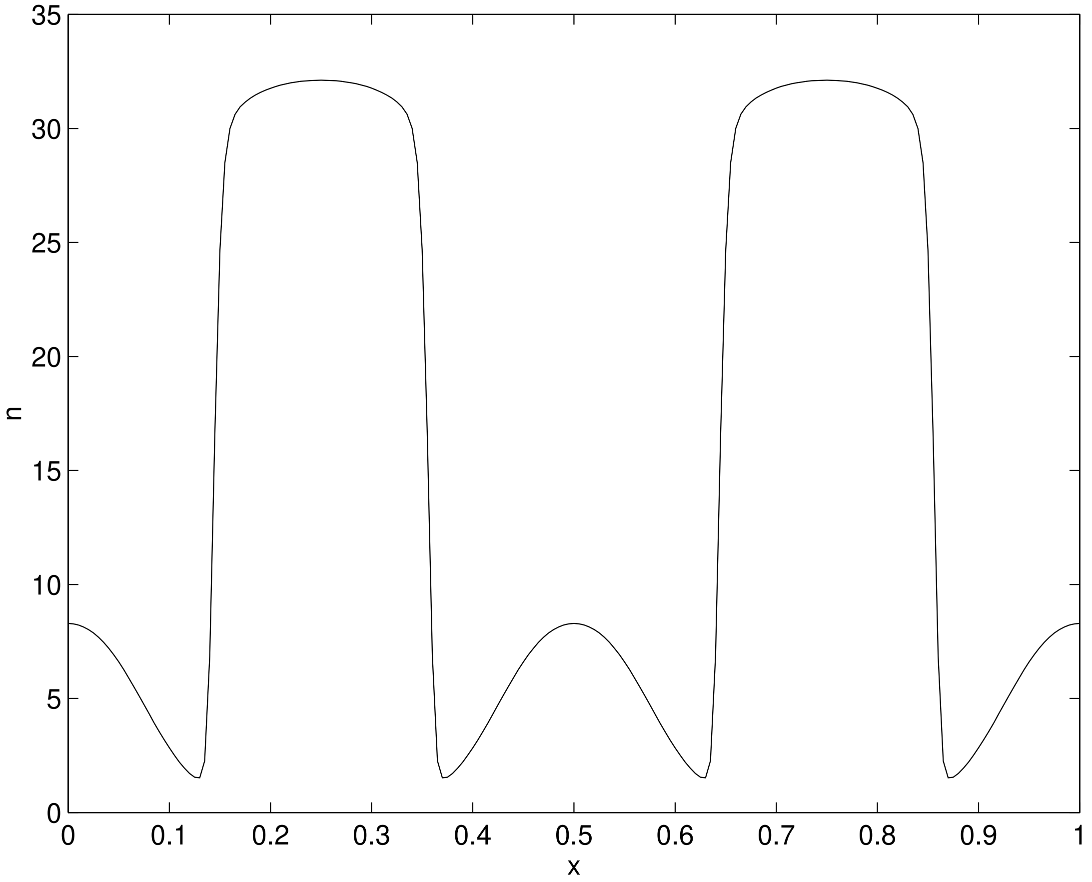

Figure 12:

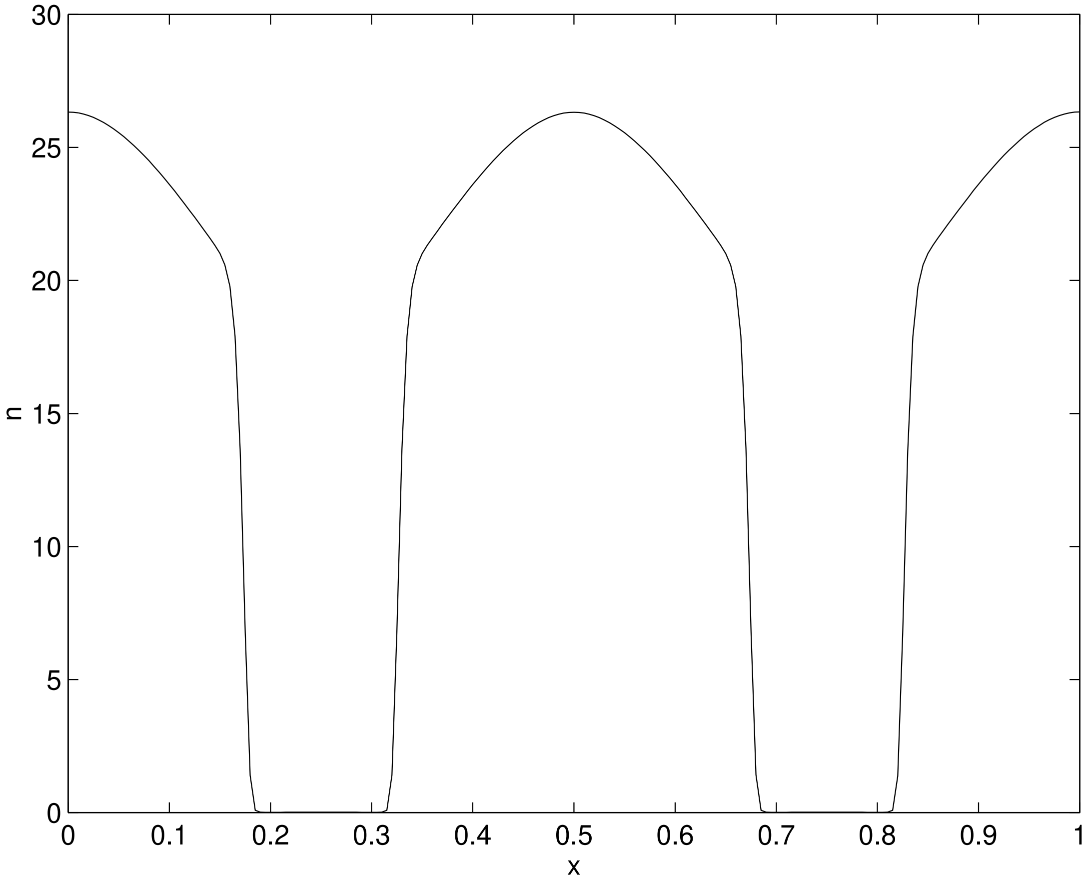

Figure 13:

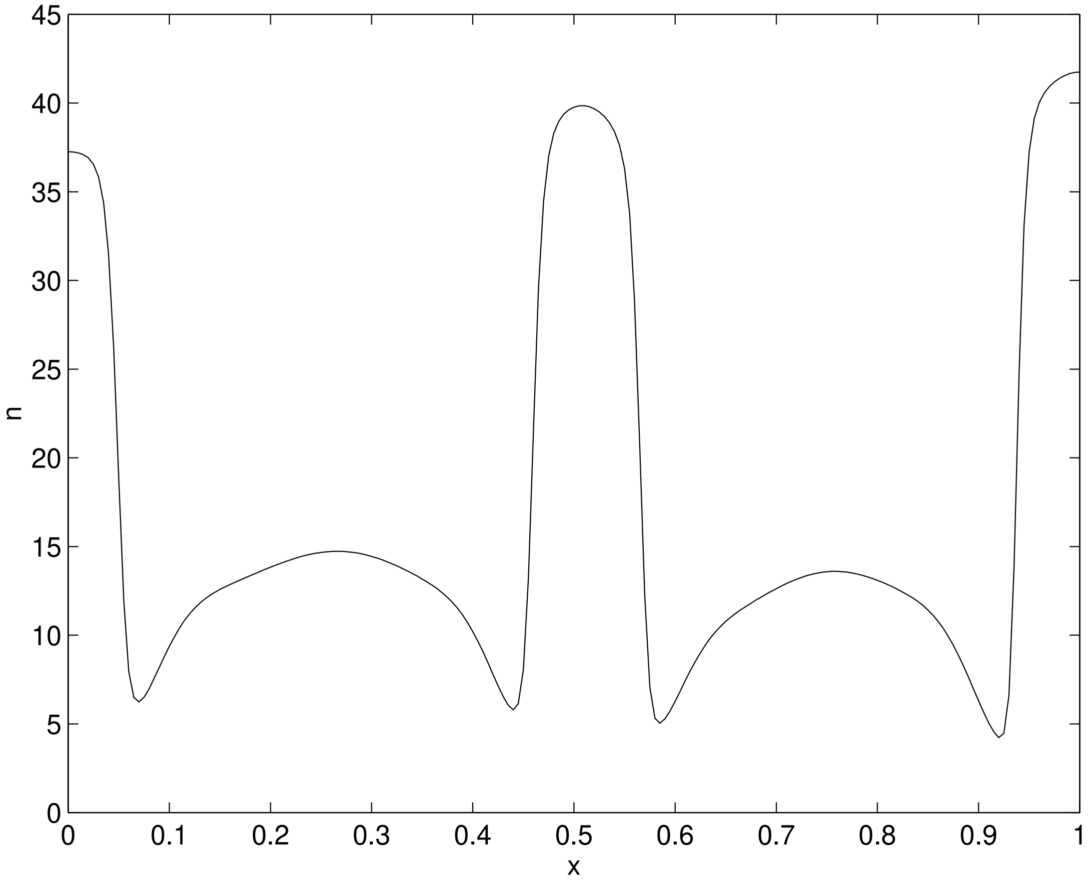

Figure 14:

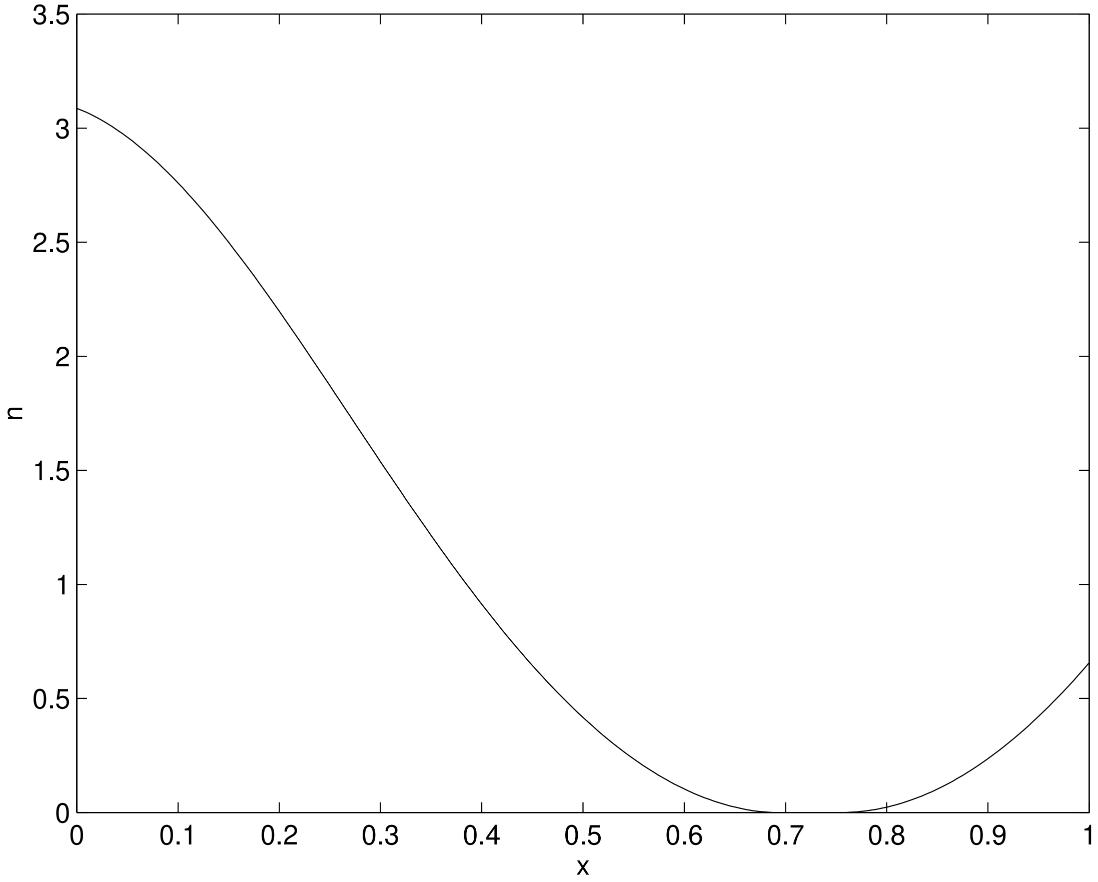

Figure 15:

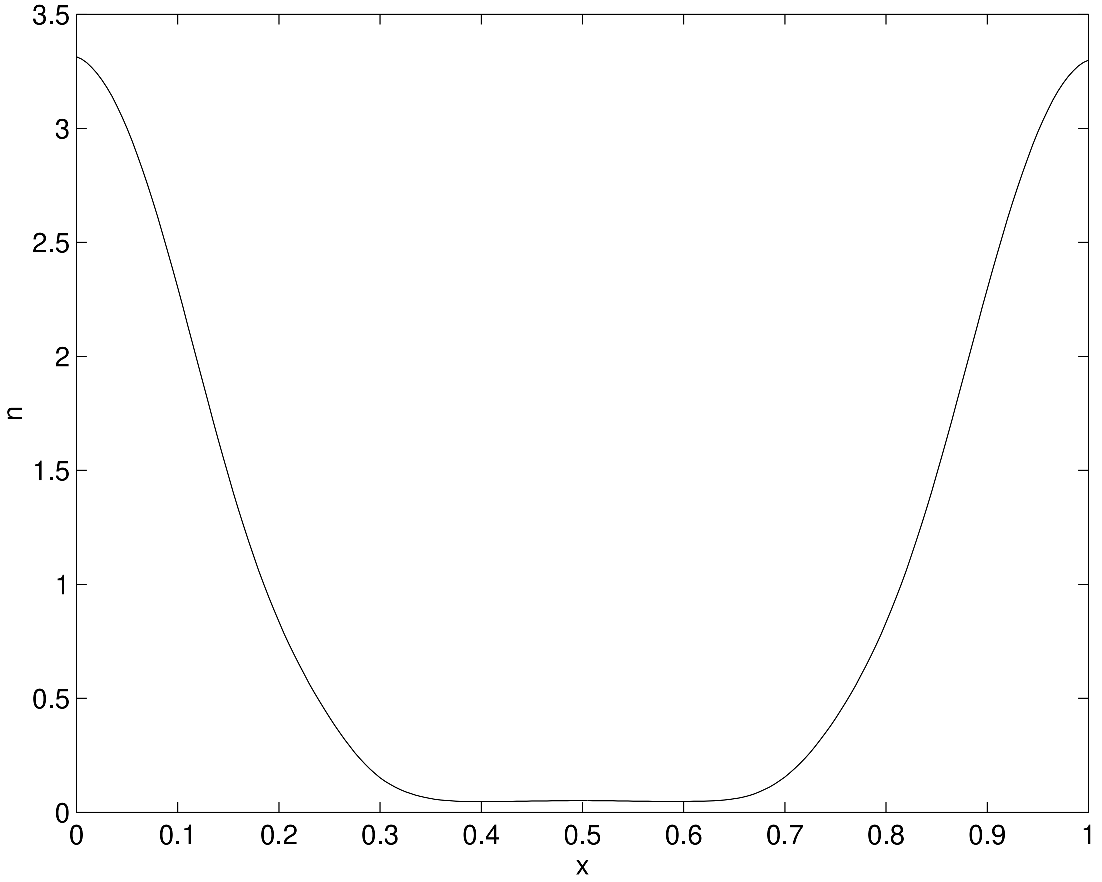

Figure 16:

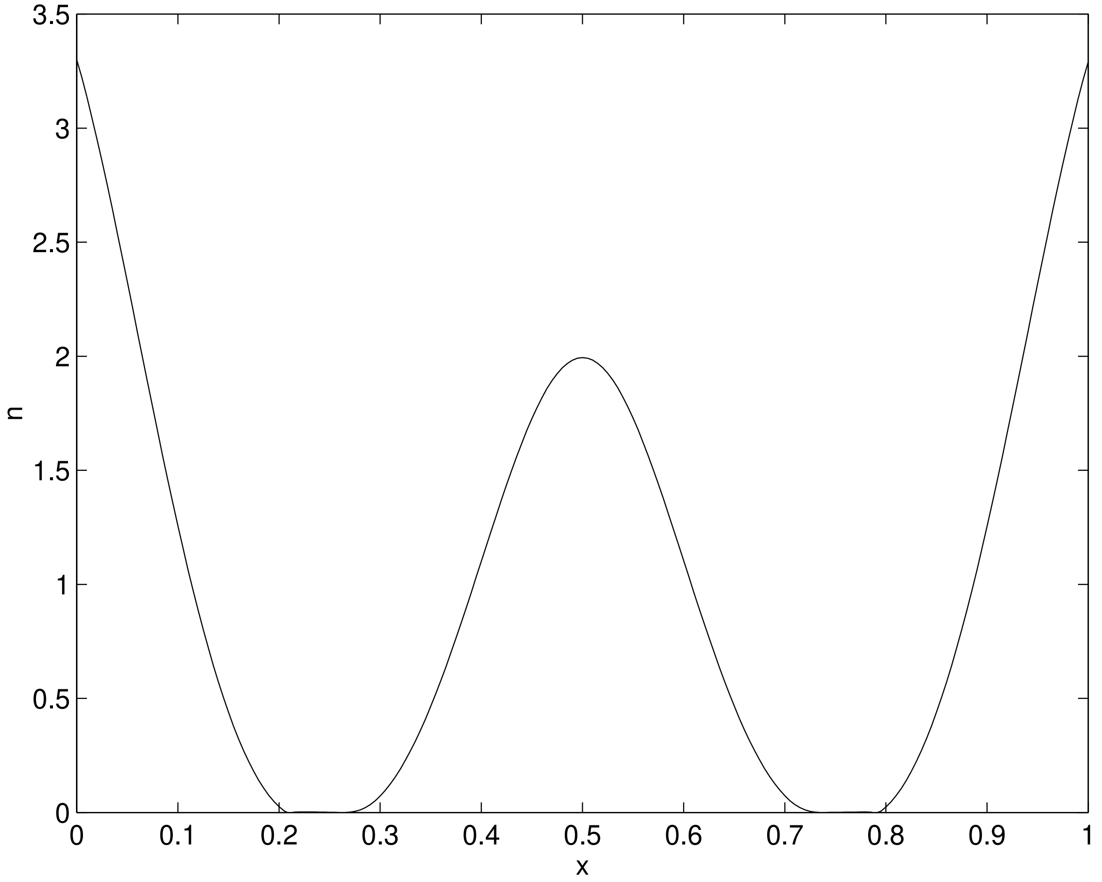

Figure 17:

References

[1] D. H. Ausprunk and J. Folkman. Migration and proliferation of endothelial cells in preformed and newly formed blood vessels during tumor angiogenesis. *Microvasc. Res.*, 14:53–65, 1977.

[2] D. Balding and D. L. S. McElwain. A. mathematical model of tumour induced capillary growth. *J. Theor. Biol.*, 114:53–73, 1985.

[3] J. C. Bowersox and N. Sorgente. Chemotaxis of aortic endothelial cells in response to fibronectin. *Cancer Res.*, 42:2547–2551, 1982.

[4] S. B. Carter. Principles of cell motility: The direction of cell movement and cancer invasion. *Nature*, 208:1183–1187, 1965.

[5] R. A. F. Clark, P. DellaPelle, E. Manseau, J. M Lanigan, H. F. Dvorak, and R. B. Colvin. Blood vessel fibronectin increases in conjunction with endothelial cell proliferation and capillary ingrowth during wound healing. *J. Invest. Dermatol.*, 79:269–276, 1982.

[6] R. A. F. Clark, J. M. Lanigan, P. DellaPelle, E. Manseau, H. F. Dvorak, and R. B. Colvin. Fibronectin and fibrin provide a provisional matrix for epidermal cell migration during wound reepithelialization. *J. Invest. Dermatol.*, 79:264–269, 1982.

[7] L. Edelstein. The propagation of fungal colonies: A model for tissue growth. *J. Theor. Biol.*, 98:679–701, 1982.

[8] A. Fenselau and R. J. Mello. Growth stimulation of cultured endothelial cells by tumor cell homogenates. *Cancer Res.*, 36:3269–3273, 1976.

[9] J. Folkman. Tumor angiogenesis. *Adv. Cancer Res.*, 43:175–203, 1985.

[10] J. Folkman and C. Haudenschild. Angiogenesis in vitro. *Nature*, 288:551–556, 1980.

[11] J. Folkman and M. Klagsbrun. Angiogenic factors. *Science*, 235:442–447, 1987.

[12] M. A. Gimbrone, R. S. Cotran, S. B. Leapman, and J. Folkman. Tumor growth and neovascularization: An experimental model using the rabbit cornea. *J. Natl. Cancer Inst.*, 52:2:413–427, 1974.

[13] L. Goldwasser, P. K. Maini, and J. D. Murray. Splitting of cell clusters and bifurcation of bryozoan branches. *J. Theor. Biol.*, 137:271–279, 1989.

[14] C. M. Goodall, A. G. Sanders, and P. Shubik. Studies of vascular patterns in living tumors with a transparent chamber inserted in hamster cheek pouch. *J. Natl. Cancer Inst.*, 35:497–505, 1965.

[15] H. T. Jarvelainen, M. Luisa Iruela-Arispe, M. G. Kinsella, L. J. Sandell, E. Helene Sage, and T. N. Wright. Expression of decorin by sprouting bovine aortic endothelial cells exhibiting angiogenesis in vitro. *Exp. Cell Res.*, 203:395–401, 1992.

[16] T. Kalebic, S. Garbisa, B. Glaser, and L. A. Liotta. Basement membrane collagen: Degradation by migrating endothelial cells. *Science*, 221:281–283, 1983.

[17] M. A. Konerding, C. van Ackern, F. Steinberg, and C. Streffer. The development of the tumour vascular system: 2-D and 3-D approaches to network formation in human xenografted tumours. In M. E. Maragoudakis, P. Gullino, and P. I. Lelkes, editors, *Angiogenesis in Health and Disease*. Plenum Press, New York, 1992.

[18] M. LaBarbera and S. Vogel. The design of fluid transport systems in organisms. *American Scientist*, 70:54–60, 1982.

[19] R. Langer, H. Brem, K. Falterman, M. Klein, and J. Folkman. Isolation of a cartilage factor that inhibits tumor neovascularization. *Science*, 193:70–72, 1976.

[20] P K Maini. Spatial and spatio-temporal patterns in a cell-haptotaxis model. *J. Math. Biol.*, 27:507–522, 1989.

[21] J. D. Murray. *Mathematical Biology.* Springer-Verlag, Berlin, 1989.

[22] V. R. Muthukkaruppan, L. Kubai, and R. Auerbach. Tumor-induced neovascularization in the mouse eye. *J. Natl. Cancer Inst.*, 69:699–704, 1982.

[23] M. R. Myerscough and J. D. Murray. Analysis of propagating pattern in a chemotaxis system. *Bull. Math. Biol.*, 54:1:77–94, 1992.

[24] G.K. Oster and J.D. Murray. Pattern formation models and developmental constraints. *J. Exp. Zool.*, 251:186–202, 1989.

[25] N. Paweletz and M. Knierim. Tumor related angiogenesis. *Crit. Rev. Oncol. Hematol.*, 9:197–242, 1989.

[26] R. W. Ruddon. *Cancer Biology*, pages 127–129. Oxford University Press, New York, 2nd edition, 1987.

[27] A.M. Schor and S.L. Schor. Tumour angiogenesis. *J. Pathol.*, 141:385–413, 1983.

[28] J. A. Sherratt and J. D. Murray. Models of epidermal wound healing. *Proc. R. Soc. Lond. B*, 241:29–36, 1990.

[29] M.M. Sholley, G. P. Ferguson, H. R. Seibel, J. L. Montour, and J. D. Wilson. Mechanisms of neovascularization. Vascular sprouting can occur without proliferation of endothelial cells. *Lab. Invest.*, 51:624–634, 1984.

[30] C. L. Stokes and D. A. Lauffenburger. Analysis of the roles of microvessel endothelial cell random motility and chemotaxis in angiogenesis. *J. Theor. Biol.*, 152:377–403, 1991.

[31] C. L. Stokes, D. A. Lauffenburger, and S. K. Williams. Migration of individual microvessel endothelial cells: stochastic model and parameter measurement. *J. Cell. Sci.*, 99:419–430, 1991.

[32] V. P. Terranova, R. DiFlorio, R. M. Lyall, S. Hic, R. Friesel, and T. Maciag. Human endothelial cells are chemotactic to endothelial cell growth factor and heparin. *J. Cell. Biol.*, 101:2330–2334, 1985.

[33] S. Ungari, R. S. Katari, G. Alessandri, and P. M. Gullino. Cooperation between fibronectin and heparin in the mobilization of capillary endothelium. *Invas. Metast.*, 5:193–205, 1985.

[34] K. M. Yamada and K. Olden. Fibronectins-adhesive glycoproteinas of cell surface and blood. *Nature*, 275:179–184, 1978.

[35] B. R. Zetter. Migration of capillary endothelial cells is stimilated by tumor-derived factors. *Nature*, 285:41–43, 1980.